

Numerical implementation of parallel electron closures in NIMROD ¹

E.D. Held and J. W. James

CEMM-APS 2001

Long Beach, CA

¹Research supported generously by the US DOE in the form of grant DE-FG03-01ER54618 and DE-FG03-01ER54660.

Heat flow involves nonlocal integration along field lines.

- The parallel heat flow definition is

$$q_{\parallel} \equiv T \int d^3v \left(\frac{v^2}{v_{th}^2} - \frac{5}{2} \right) v_{\parallel} f.$$

- Heat flow moment appears as drive:

$$\begin{pmatrix} \nu & v\epsilon_{0,1}\frac{\partial}{\partial L} & 0 & 0 & \dots \\ v\epsilon_{1,0}\frac{\partial}{\partial L} & \lambda_1\nu & v\epsilon_{1,2}\frac{\partial}{\partial L} & 0 & \dots \\ 0 & v\epsilon_{2,1}\frac{\partial}{\partial L} & \lambda_2\nu & v\epsilon_{2,3}\frac{\partial}{\partial L} & 0 & \dots \\ \vdots & \vdots & \vdots & \vdots & \vdots & \vdots \\ \dots & \dots & \dots & 0 & v\epsilon_{N,N-1}\frac{\partial}{\partial L} & \lambda_N\nu \end{pmatrix} \begin{pmatrix} F_0 \\ F_1 \\ F_2 \\ \vdots \\ F_N \end{pmatrix} = \begin{pmatrix} -\frac{4}{3}L_1^{(\frac{1}{2})}\frac{\partial q_{\parallel}}{\partial L}\frac{f_M}{p} \\ \frac{2}{3}vL_1^{(\frac{3}{2})}\frac{\partial T}{\partial L}\frac{f_M}{T} \\ 0 \\ \vdots \\ 0 \end{pmatrix}$$

- Explicit treatment using q_{\parallel} and T at previous timestep.

$$q_{\parallel}^{n+1}(L') = \int^{L'} dL [T^n(L' - L) - T^n(L' + L)] \frac{\partial K_{q_{\parallel}}}{\partial(\ln L)} + G(q_{\parallel}^n(L')),$$

$$K(s, L_{mfp}) = n_0 v_{th} s^3 \left(s^2 - \frac{5}{2} \right)^2 \sum_{i=0}^N a_i \exp(-s^2 - \bar{k}_i L).$$

Collisional information contained in effective mean free paths, k 's.

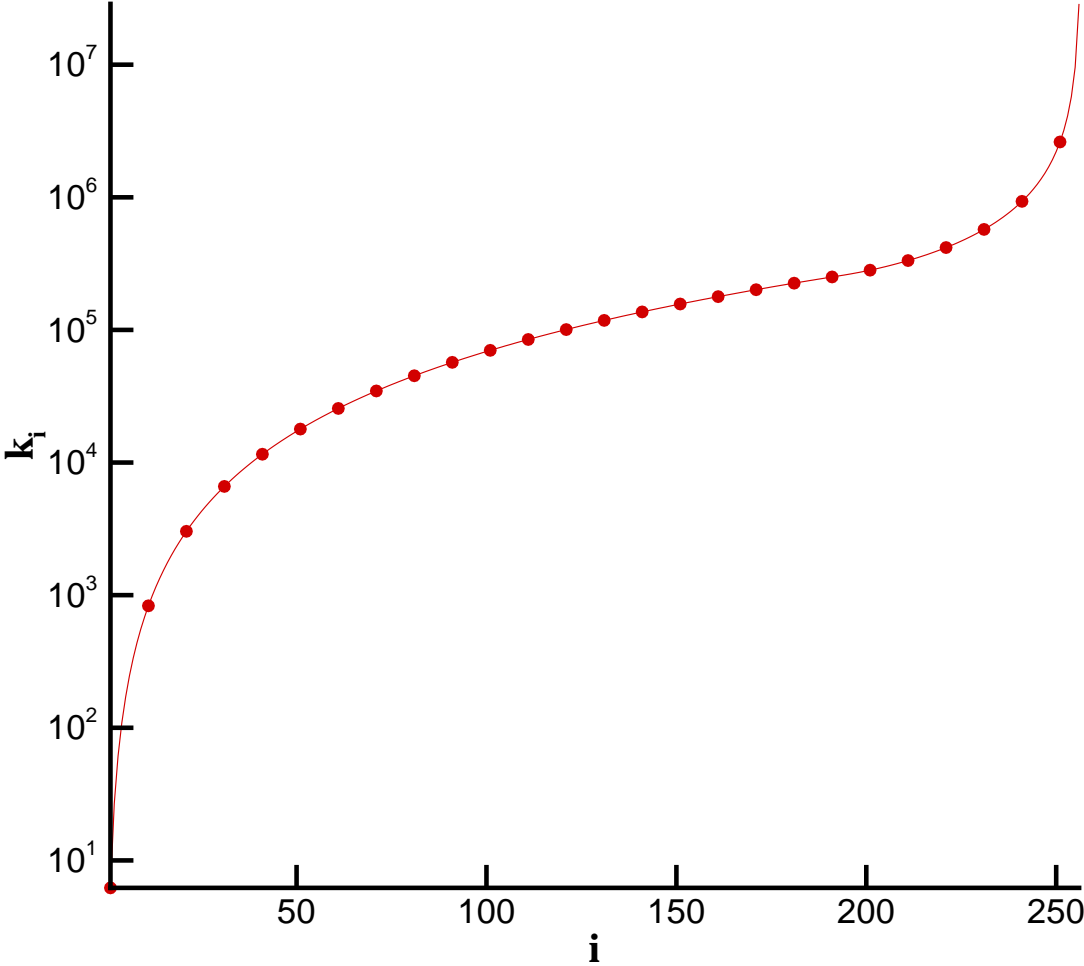


Figure 1: k_i 's resulting from expansion in basis of 512 Legendre polynomials.

Collisional information contained in coefficients, a_i 's.

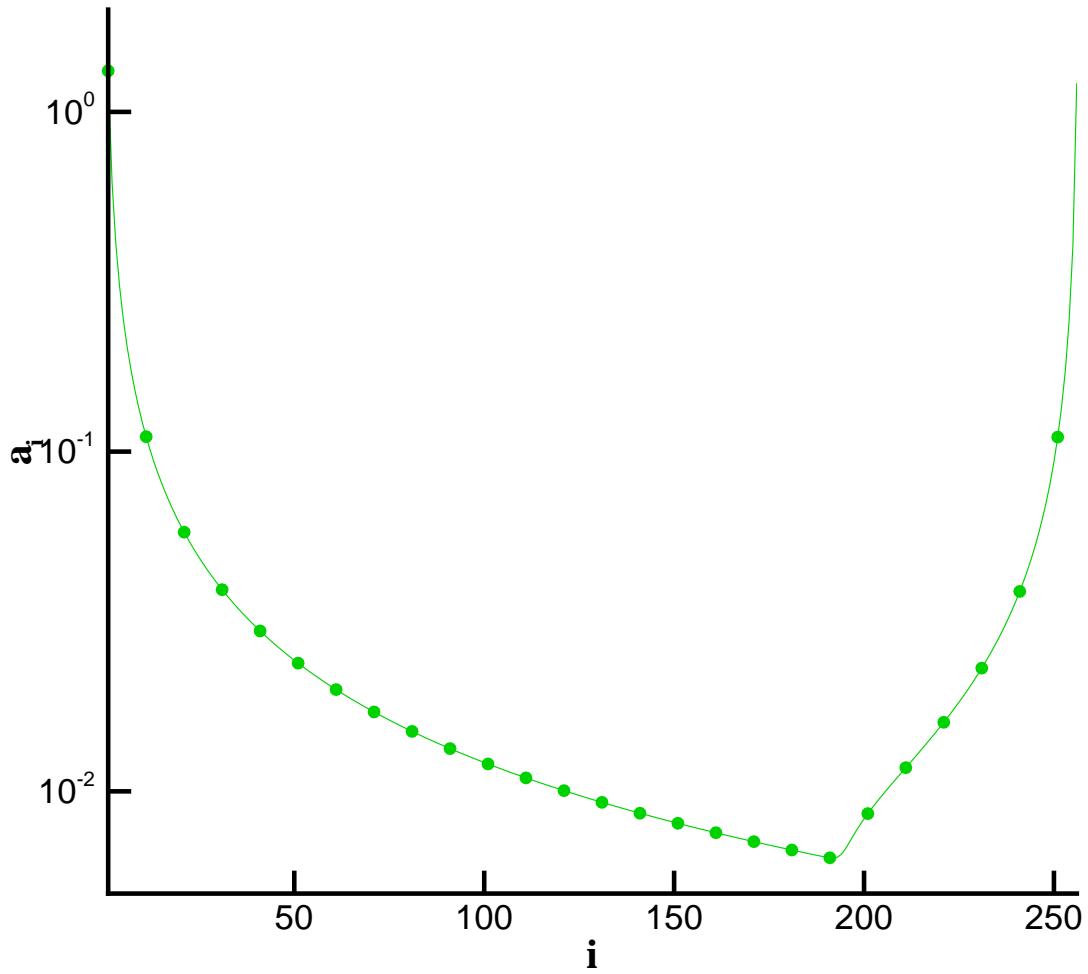


Figure 2: a_i 's resulting from expansion in basis of 512 Legendre polynomials.

Heat flux closure approximate for arbitrary collisionality.

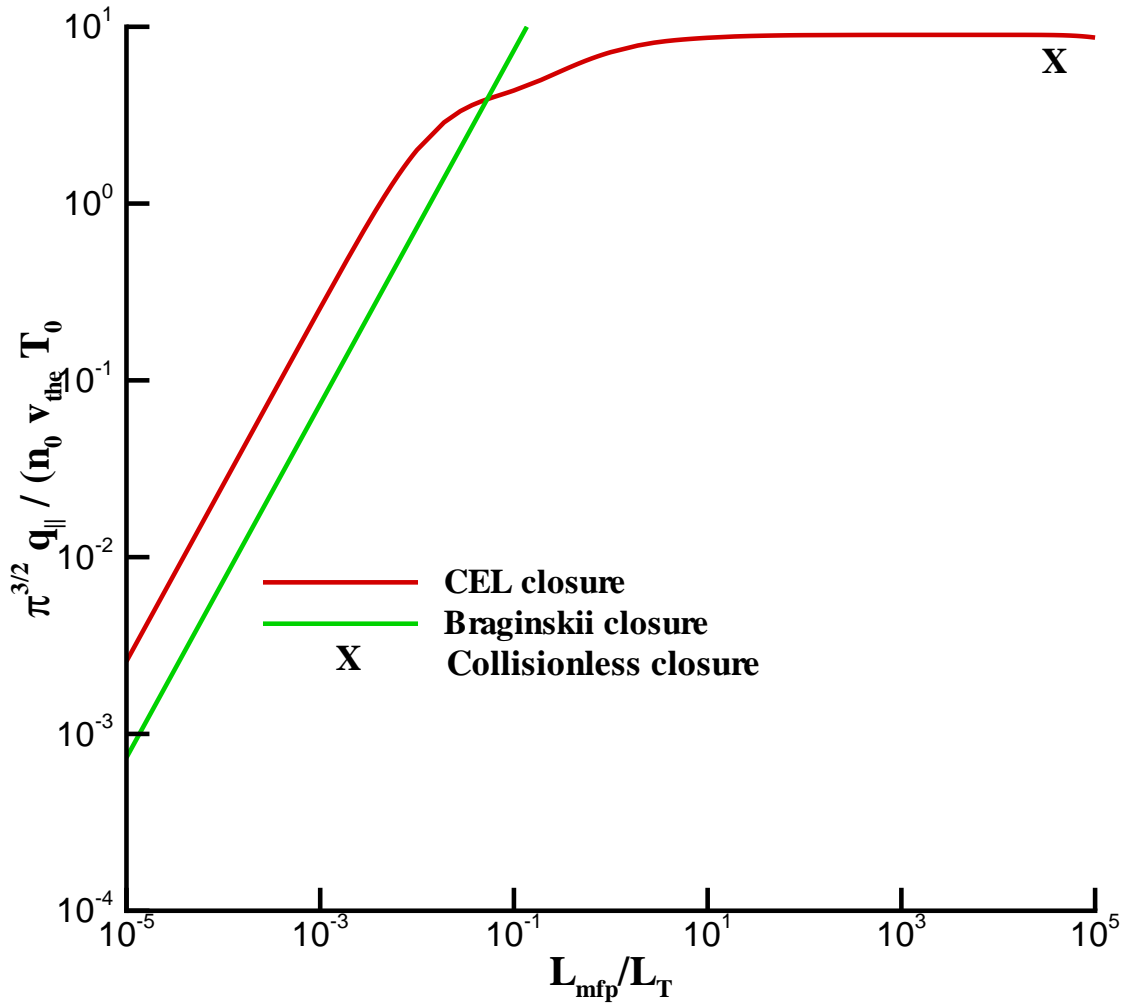


Figure 3: Heat flux for homogeneous magnetic field and sinusoidal temperature perturbations.

Nearly collisionless closure truncates more rapidly than collisionless closure.

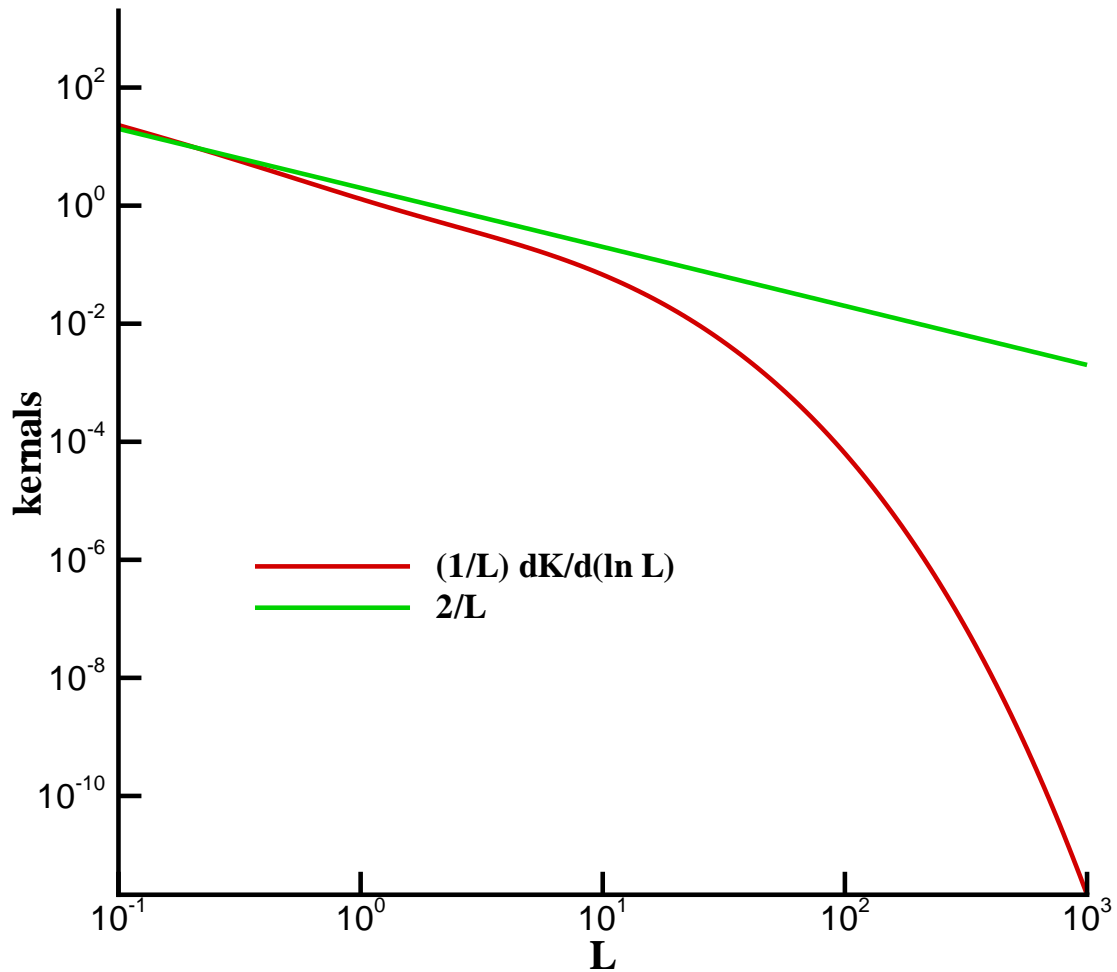


Figure 4: Kernel of nearly collisionless closure falls off more rapidly than kernel of collisionless closure. Here it was assumed that $L_{mfp} = 1$.

*Islands in slab geometry good testbed for
heat flux closures.*

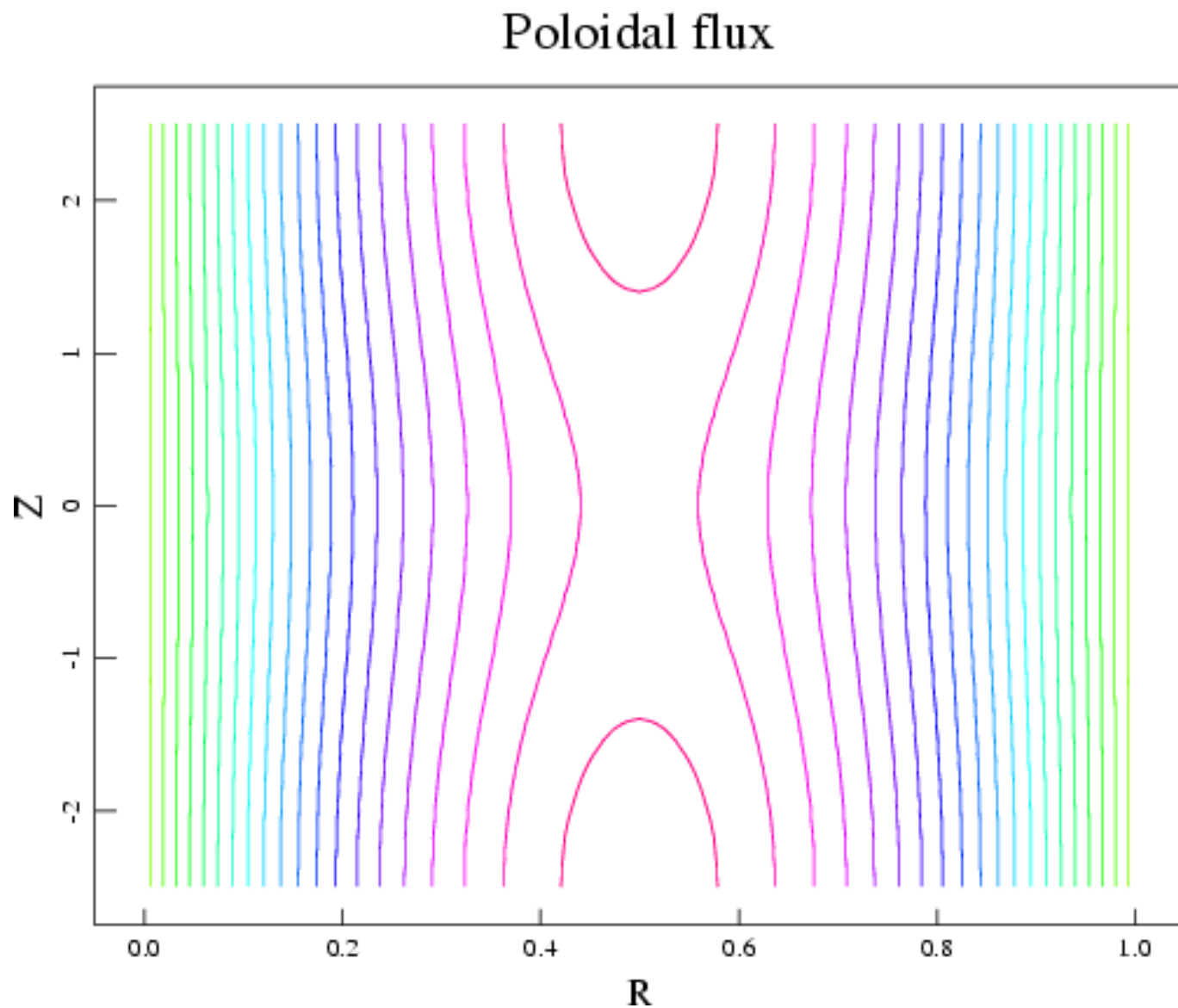


Figure 5: Single-helicity island in slab geometry periodic in Z and into plane.

Parallel heat flow added as vector field to NIMROD.

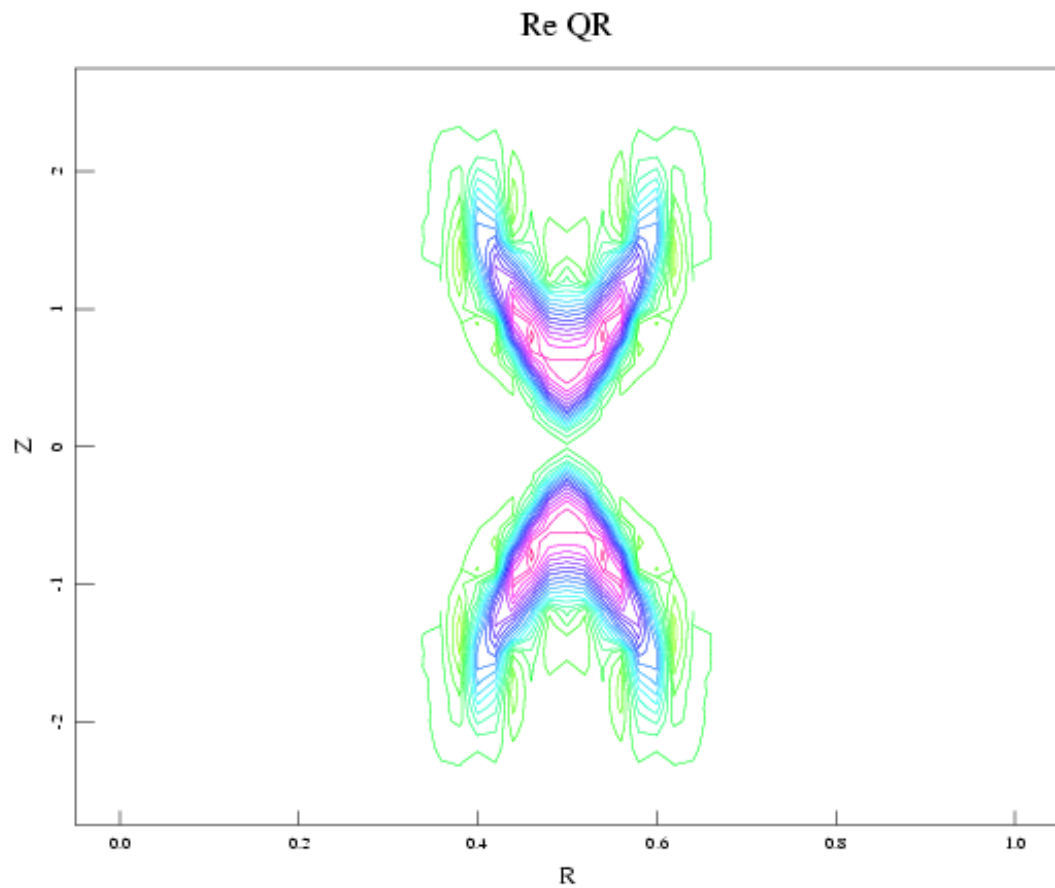


Figure 6: Radial component of flow of heat inside island due to rapid free-streaming/diffusive transport along field lines.

Diffusive and CEL closures take different forms.

- Diffusive heat flow uses

$$\vec{\nabla} \cdot \vec{q} = \vec{\nabla} \cdot \kappa \vec{\nabla} T = \kappa_{\perp} \nabla^2 T + \vec{\nabla} \cdot (\kappa_{\parallel} - \kappa_{\perp}) \hat{b} \hat{b} \cdot \vec{\nabla} T,$$

where κ_{\parallel} and κ_{\perp} are the parallel and perpendicular scalar conductivities.

- CEL closure can be written in several different forms:

$$\vec{\nabla} \cdot \vec{q} = \kappa_{\perp} \nabla^2 T - \vec{\nabla} \cdot \kappa_{\perp} \hat{b} \hat{b} \cdot \vec{\nabla} T + \vec{\nabla} \cdot \vec{q}_{\parallel},$$

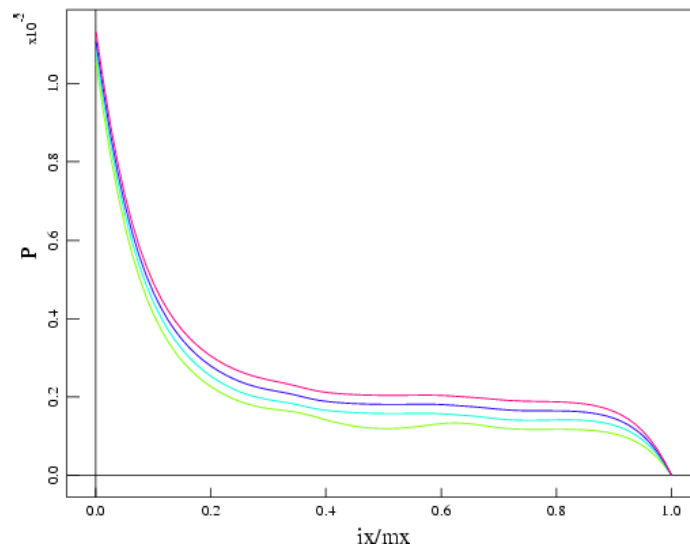
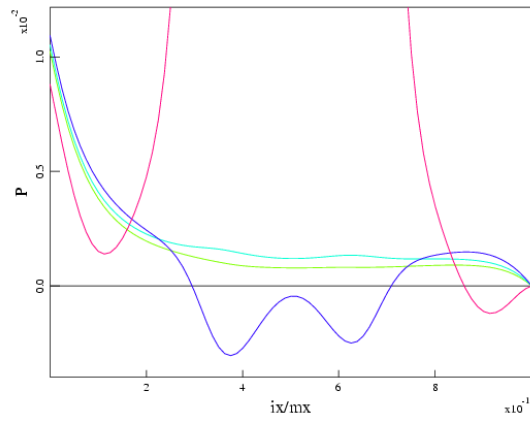
where $\vec{q}_{\parallel} = q_{\parallel} \hat{b}$ hence,

$$\vec{\nabla} \cdot \vec{q}_{\parallel} = \hat{b} \cdot \vec{\nabla} q_{\parallel} + q_{\parallel} \hat{b} \cdot \vec{\nabla} \hat{b}.$$

- Pressure equation stabilized numerically with self-adjoint, semi-implicit operator on left side.

$$\left[\mathbf{I} - dt f \left(\kappa_{\perp} \nabla^2 + \vec{\nabla} \cdot (\kappa_{\parallel} - \kappa_{\perp}) \hat{b} \hat{b} \cdot \vec{\nabla} \right) \right] \Delta T = dt \left[\kappa_{\perp} \nabla^2 T - \vec{\nabla} \cdot \kappa_{\perp} \hat{b} \hat{b} \cdot \vec{\nabla} T + \vec{\nabla} \cdot \vec{q}_{\parallel} \right]$$

Semi-implicit operator critical for numerical stability.



Parallel heat flow robustly flattens pressure across O-point.

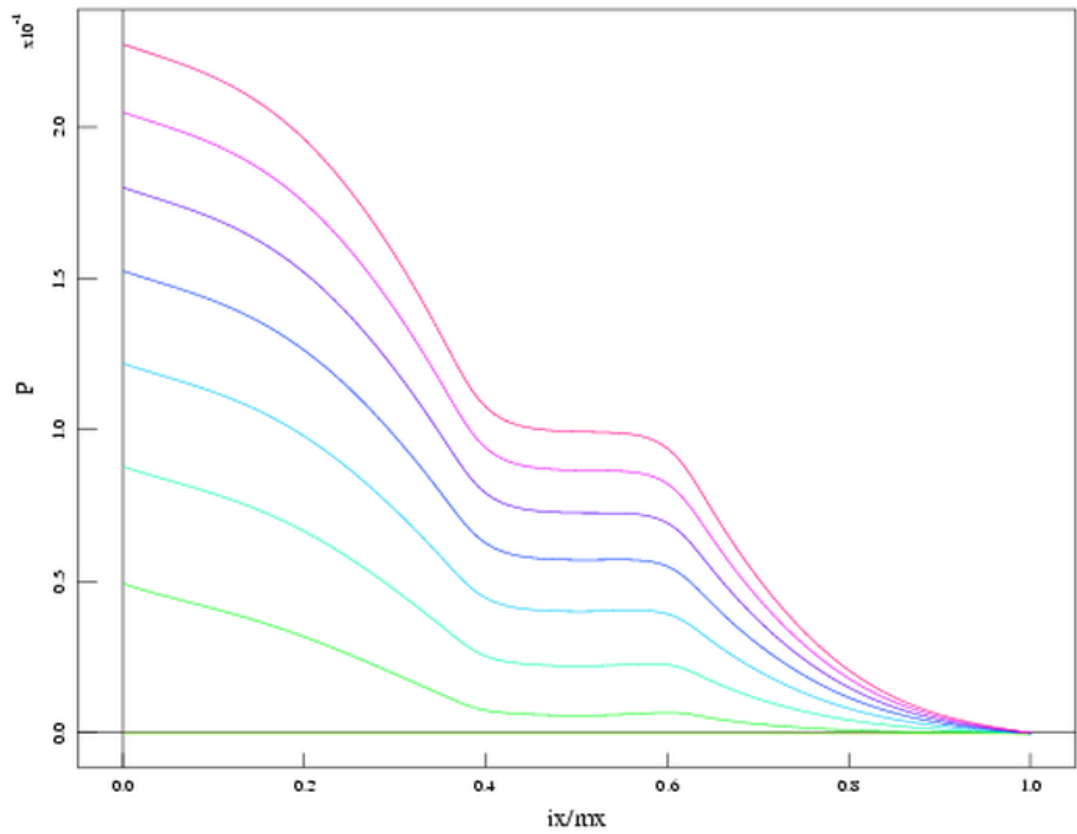


Figure 7: Flattening inside island due to rapid free-streaming/diffusive transport along field lines.

Conclusions

- Robust temperature flattening from CEL heat flow closure.

10^2 larger parallel heat flow with $v_{the}/\pi^{3/2} \sim 10^6$ and $n_e = 5 \times 10^{13}$ in CEL model compared to diffusive model with $\kappa_{\parallel} = 10^7$.

- Processors integrate $\approx 10^2 - 10^3$ m for single heat flux calculation to converge.

$$T_e = 100\text{eV}, v_{the} = 5 \times 10^6 \text{ and } L_{mfp} = 2 - 3\text{m}.$$

- CEL heat flow time $>$ pressure equation solve time

100 processors on 40 X 40 grid and cubic finite elements spend 80% of CPU time on CEL closures

- More work needed for production runs.